A Cable-Suspended Intelligent Crane Assist Device for the Intuitive Manipulation of Large Payloads

Article *in* IEEE/ASME Transactions on Mechatronics · August 2016

DOI: 10.1109/TMECH.2016.2531626

5 authors, including:

Alexandre Campeau-Lecours
Laval University
18 PUBLICATIONS **40** CITATIONS

SEE PROFILE

Clément Gosselin
Laval University
500 PUBLICATIONS **13,277** CITATIONS

SEE PROFILE

A cable-suspended intelligent crane assist device for the intuitive manipulation of large payloads

This paper is a Post-Print version (ie final draft post-refereeing). For access to Publishers version, please access 10.1109/TMECH.2016.2531626.

Alexandre Campeau-Lecours, *Member, IEEE,* Simon Foucault, Thierry Laliberté, Boris Mayer-St-Onge, and Clément Gosselin, *Fellow, IEEE*

***Abstract*—This paper presents a cable-suspended crane system to assist operators in moving and lifting large payloads. The main objective of this work is to develop a simple and reliable system to help operators in industry to be more productive while preventing injuries. The system is based on the development of a precise and reliable cable angle sensor and a complete dynamic model of the system. Adaptive horizontal and vertical controllers designed for direct physical human-robot interaction (pHRI) are then proposed. Different techniques are then proposed to estimate the payload acceleration in order to increase the controller performances. Finally, experiments performed on a full-scale industrial system are presented.**

Index terms: Human-robot interaction; Robotic assembly; Force control; Assistive technology; Command and control systems.

I. INTRODUCTION

Assistive devices are used in many industrial applications to help operators moving and lifting payloads. The objective of such devices is to combine the force capabilities of the robot with the decision and adaptation capabilities of the human operator. This approach allows to perform tasks that would be too complex or demanding for automated systems alone or that would be too dangerous and prone to injuries for a human operator. Such systems are often referred to as Intelligent Assist Devices (IAD) and are used in many industrial applications [1].

Typical augmentation systems require the operator to interact through an instrumented handle attached to the device. However, because the payload is often far from the handle, such an arrangement makes the performance of some tasks not necessarily intuitive. In order to alleviate this drawback, assistive devices in which the operator can place his hands directly on the payload have been developed [1]. By being in close contact with the payload, it is easier to manipulate and to guide the assistive device. The operator can also change his hands position to be more efficient, productive, comfortable or to have a clearer view of the task at hand. Similarly, the operator can also use only one hand while the other is used for another aspect of the task [2], [1]. Finally, this arrangement allows several operators to interact with a same payload.

While many human augmentation systems use rigid link mechanisms, it is common in industrial practice to support a payload from a cable. The resulting systems are simpler, they allow free rotation, they have a reduced inertia and cost and they lead to a less cumbersome structure [1]. Although the centre of mass of the payload is necessarily aligned with the cable, this is not a major concern for many applications.

Typical cable-suspended systems allow passive motions in the horizontal plane. As a consequence, the operator must still impart a large force to move the payload. It is usually even more difficult to stop the payload, which tends to oscillate, and this can result in potential injuries [1]. In order to alleviate this drawback, a servo-controlled cable suspended lift assist device controlled with a sliding handle was developed [3], [1]. In order for the operator to be able to place his hands anywhere on the payload to impart a motion, a cable angle sensor can be integrated to the system [1], [4], [5] in order to detect cable deviation from the vertical and then to assist the operator in the horizontal plane [6], [7], [8]. In order to offer the same assistance in the vertical direction, a force sensor is normally placed in line with the cable. However, the force signal is affected by the dynamical effects of the payload [3], [8] which must then be compensated for in order to obtain a good estimation of the force applied by the operator [9], [10]. The resulting signal is then used as an input to a force control scheme such as admittance control [11] to assist the operator in moving the payload [8], [12].

In order to improve the assistance to the operator, different control schemes for human assistance were also proposed such as estimating the operator force to implement an impedance control scheme [7], using neural networks to vary the controller parameters online [12] and improving the estimation of the force applied by the operator [13]. More detailed literature reviews are presented in each individual section of the paper.

The main objective of this work is to improve the performances and the intuitiveness of cable-suspended intelligent crane assist devices. In contrast to the previous work, this paper proposes a novel concept of cable angle sensor and a new control structure for the horizontal and vertical assistance

This work was supported by The Natural Sciences and Engineering Research Council of Canada (NSERC) as well as by the Canada Research Chair Program and General Motors (GM) of Canada.

The authors are with the Department of Mechanical Engineering, Université Laval, Québec, Canada. Contact e-mail: alexandre.campeau-lecours@gmc.ulaval.ca

Fig. 1: Prototype of the cable-suspended assistive device proposed in this work.

control. The proposed cable angle sensor is designed to be reliable (for industrial applications), low-cost and accurate (in order to decrease the force required by the operator). Based on well known cable-based crane system controllers, an horizontal controller is adapted to the context of human assistance in order to provide assistance to the operator to move the payload by automatically computing stable control gains for any cable length. Based on admittance control and previous litterature, the proposed vertical controller increases the precision of the dynamical effects estimation and allows to reduce the force required by the operator to move the payload. Finally, experiments performed on an industrial-scale prototype (shown in Fig. 1) are presented.

II. CABLE ANGLE SENSOR

Cable-suspended assistive devices usually use a cable angle sensor or a force sensor to infer human intentions [1], [4], [14], [15], [7]. In many applications, the extension of the cable is measured using a simple encoder attached to a reel. However, it is much more challenging to measure the inclination of the cable and over the years, different solutions have been proposed. Amongst them is a non-contact sensor using an AC magnetic field [4], accelerometers placed on the cable (used as inclinometers) [16], machine vision [17], [18], a cardan-based mechanism [19], a linear cable displacement sensor [5] and observer based solutions [20]. The sensor requirements are robustness (for industrial applications), accuracy, simplicity and low cost. Observer based solutions were thus rejected for lack of robustness. Non-contact sensors (which are sensitive to electromagnetic disturbances), accelerometers placed on the cable (affected by noise, drift and dynamical effects) and machine vision (difficult to implement in practice especially if the camera view is blocked) were also left aside for robustness consideration. A contact sensor using encoders is thus preferred since it represents a proven robust solution in industry. Amongst existing contact based sensors, cardan based mechanisms [19] and a sensor detecting the horizontal displacement of the cable [5] were also left aside since such mechanisms are affecting the dynamics and the measurement precision by creating a break point on the cable and because parts interference limit the achievable workspace. A contact sensor (see patent [21]) was thus designed to alleviate these problems as detailed in the next section.

A. SENSOR DESCRIPTION

A cable angle sensor using concentric grooved parts is proposed here. The cable passes through the parts and drives them as it moves, as shown in Fig. 2. The concentric parts, which move independently from one another, are each attached to two shafts and the cable angles are obtained by measuring the shaft rotations. Similar mechanisms were used for other applications such as a spherical robot wrist [22] and early computer joysticks [23]. Measuring a shaft rotation is very common in industrial practice thus leading to a robust measurement of the cable angle. This cable angle sensor mechanism is part of the material described in a patent [21]. The resolution for this prototype is 0.09 degree. Similarly to other contact sensors, the effects of the sensor mechanism on cable dynamics are negligible because the moving parts are very lightweight ($0.06\ kg$) compared to the payload (minimum of $3\ kg$), friction is low and the moving parts are close to the cable pivot point.

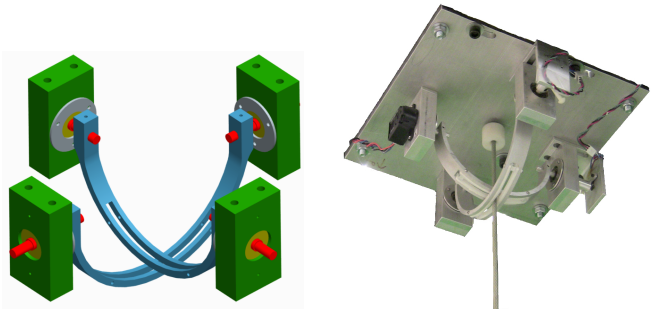

(a) CAD model of the cable angle sensor.

(b) Prototype of the cable angle sensor.

Fig. 2: Cable angle sensor CAD model and prototype.

Because there are two shafts per axis and two sides per shaft, several sensors can be used, such as relative encoders, Hall effect sensors, absolute encoders, potentiometers, accelerometers, gyroscopes and photointeruptors. In this paper, an encoder and a Hall effect sensor are used for each axis. Although only one sensor per axis is enough, the pair encoder-Hall effect sensor is useful for many reasons. First, the signals can be combined using data fusion to obtain a signal of better quality. Secondly, it is possible to compare both signals in order to detect problems. Finally, this arrangement takes advantage of the absolute signal of the Hall effect sensor while taking advantage of the encoder precision. In the experiments, the encoder and Hall Effect sensor signals are fused using a Kalman filter. Two models are used: a linearized model based on the cable dynamics and a third order acceleration model [24]. This data fusion allows to obtain position and velocity signals of better quality which is very important for control purposes.

B. CABLE ANGLE PROCESSING

When implementing control algorithms, practical issues arise. For example, a deadband on the cable angle is normally used in order to be robust to small cable angle measurement errors [6]. Another issue also arises from small amplitude

and high frequency oscillations of the cable originating from different vibration modes.

The controller must not damp these oscillations but it must be robust to their effects. Usually, the deadband is increased to cope with this problem, at the expense of accuracy [6]. Another option is to implement a low pass filter, but this adds delay and can lead to instability. An algorithm is proposed here to filter these oscillations while keeping precision and performances.

A deadband ($\theta_{db1} = 1°$) is first applied on the input angle (θ_{in}) to obtain the angle (θ_{p1}):

$$\theta_{p1} = \begin{cases} 0 & \text{if } -\theta_{db1} < \theta_{in} < \theta_{db1} \\ \theta_{in} - \theta_{db1} & \text{if } \theta_{in} > \theta_{db1} \\ \theta_{in} + \theta_{db1} & \text{if } \theta_{in} < -\theta_{db1} \end{cases} . \quad (1)$$

The absolute signal of θ_{p1} then passes through a rate limiter where the rising limit is low and the falling limit is high. It thus takes time for the output signal to increase, filtering high frequency oscillations, but it can return to zero rapidly, thus avoiding phase shift. This signal is then multiplied by the sign of θ_{p1}. This algorithm simply reproduces a rate limiter in which the magnitude of the signal takes more time to increase from zero but can rapidly go back towards zero. An example result is shown in Fig. 3 were no deadband ($\theta_{db1} = 0$) was implemented in order to have a better understanding of the filter alone. The algorithm filters small amplitude and high frequency oscillations while allowing to use a smaller deadband and avoiding the delays obtained from typical low pass filters. In this example, the filter was applied to the whole input signal. However, it is also possible to apply the filter only to a small part of the signal.

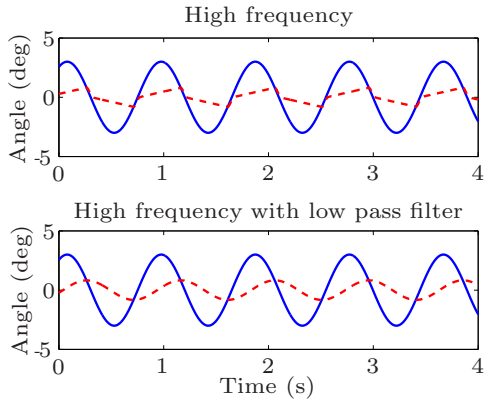

Fig. 3: Example output obtained with the proposed rate-limiter filter. The solid line is the angle input while the dashed line is the filter output. The result obtained with a standard low-pass filter is provided for comparison purposes.

III. DYNAMICS

In the following, the model parameters and equations of motion are developed. The equations of motion are first obtained with a complete model referred to as *coupled motion* and then, with simplifications, a *simplified model* is obtained.

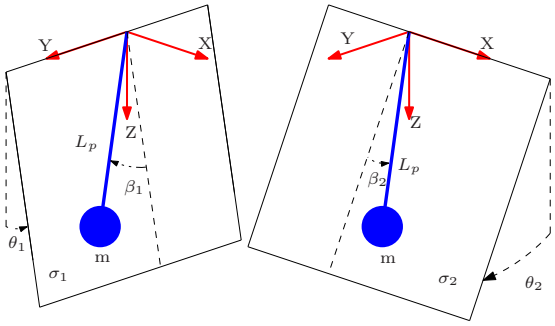

Fig. 4: Definition of the parameters used in the dynamic model.

A. COUPLED MOTION

1) ANGLE REPRESENTATION: The parameters used to describe the kinematics of the cable are shown in Fig. 4. The measured variables from the cable angle sensor are θ_1 and θ_2 and correspond to the rotations about the Y axis (in the XZ plane) and X axis (in the YZ plane) respectively. From Fig. 4, a plane σ_1 is defined using the Y axis and the payload position. Angle β_1 is defined as the angle between the direction of the cable and the direction normal to the Y axis and contained in plane σ_1 [25].

2) EQUATIONS OF MOTION: The equations of motion are [25]:

$$\begin{aligned} F_x &= M_x\ddot{X}_c + m(\ddot{X}_c + \ddot{L}_p c\beta_1 s\theta_1 - L_p\ddot{\beta}_1 s\beta_1 s\theta_1 \quad (2) \\ &\quad -L_p\dot{\beta}_1^2 c\beta_1 s\theta_1 - L_p\dot{\theta}_1^2 c\beta_1 s\theta_1 + 2\dot{L}_p\dot{\theta}_1 c\beta_1 c\theta_1 \\ F_y &= M_y\ddot{Y}_c + m(\ddot{Y}_c + 2\dot{L}_p\dot{\beta}_1 c\beta_1 - L_p\dot{\beta}_1^2 s\beta_1 \\ &\quad +L_p\ddot{\beta}_1 c\beta_1 + \ddot{L}_p s\beta_1) \quad (3) \\ F_l &= m(\ddot{X}_c c\beta_1 s\theta_1 + \ddot{L}_p + \ddot{Y}_c s\beta_1 - L_p\dot{\beta}_1^2 \\ &\quad -L_p\dot{\theta}_1^2 c^2\beta_1 - gc\beta_1 c\theta_1) \quad (4) \\ 0 &= mL_p c\beta_1(L_p\ddot{\theta}_1 + \ddot{x}c\theta_1 + gs\theta_1 + 2\dot{L}_p\dot{\theta}_1 c\beta_1 \\ &\quad -2L_p\dot{\theta}_1\dot{\beta}_1 s\beta_1) \quad (5) \\ 0 &= mL_p(L_p\ddot{\beta}_1 + L_p\ddot{y}c\beta_1 - \ddot{x}s\beta s\theta + 2\dot{\beta}_1\dot{L}_p \\ &\quad +L_p\dot{\theta}_1^2 c\beta_1 s\beta_1 + mgs\beta_1 c\theta_1) \quad (6) \end{aligned}$$

where the prefixes s and c (as in $s\beta$) represents sin and cos respectively, m is the mass of the payload (which is considered to be a point-mass), M_x is the cart effective mass in the X direction and M_y the cart effective mass in the Y direction[1], X_p, Y_p and Z_p are the Cartesian coordinates of the payload's centre of mass in fixed coordinates, X_c and Y_c are the cart coordinates, L_p is the distance between the cable pivot point and the payload centre of mass, F_x is the X axis trolley force, F_y is the Y axis trolley force, F_l is the tension in the cable, the last two equations represent the pendulum oscillations. The cable mass is neglected. Globally, the system has five degrees of freedom (if the payload is assumed to be a point mass) and three controlled inputs. Similar and equivalent equations could be found with other angle representations such as (θ_2,β_2). From eqns. (2) to (6) and namely eqn. (5), it can be seen that the coupling between the angles is negligible for relatively

[1]The effective mass of the cart can be different in each direction since a bridge and trolley system is typically used to move in the horizontal plane.

small angles and small angular velocities. Thus, neglecting the coupling effects, a simplified model can be obtained in which the X and Y motions are treated separately, as shown in the next section.

B. SIMPLIFIED MODEL

Considering only one degree of freedom (X axis), and assuming small angles, a relatively slowly varying cable length and neglecting $\dot{\theta}_1^2$, the equations can be linearized as [25]:

$$F_x = (M_x + m)\ddot{x} + m\ddot{\theta}_1 L_p \quad (7)$$

$$0 = \ddot{x} + g\theta_1 + L_p\ddot{\theta}_1. \quad (8)$$

where M_x is the cart mass is the X direction, m is the payload mass and where L_p is considered constant over a time step.

IV. HORIZONTAL MOTION CONTROL

In this section, two horizontal control modes are presented, namely the cooperation mode and the autonomous mode. In both cases, the system measures the cable angle and the controller's objective is to keep the cable vertical by moving the overhead cart. In the cooperation mode, the operator imparts an angle to the cable by pushing on the payload. The controller thus moves the overhead cart in the direction desired by the operator, while controlling cable sway, resulting in an intuitive assistance to the operator. Additionally, since the controller's objective it to maintain the cable vertical, the operator does not need to stop the load himself, which could otherwise raise ergonomic issues. Finally, in the autonomous mode, the cart is moving by itself to reach a prescribed position while controlling cable sway.

A. OVERVIEW

The problem of controlling the position or speed of a cart-pendulum system while damping the payload oscillations has been extensively explored in the literature. In usual applications, the crane position is controlled in autonomous mode or remotely by an operator. The control objectives are usually to obtain good positioning accuracy, to reduce the payload oscillations caused by the overhead crane motions and to eliminate oscillations induced by external disturbances [17]. In a human assistance context, the deviation of the cable from the vertical is not due to a disturbance but is the main input from the operator. The controller must not only be stable but must also result in smooth and intuitive motions to the human operator. Control strategies must then be adapted to the context of this problem.

A well-known method for controlling cable sway is input shaping, where the reference signal is convolved with a sequence of impulses to eliminate sway in an anticipatory way [17]. Other methods include state-space control [26], [16], backstepping [27], Lyapunov stability analysis [28], passivity [29] or proportional derivative control laws [30]. These controller were designed to control the position of the cart while minimizing cable oscillations. However, in a direct assistance context, there is no prescribed position and the above mentioned controllers could not be applied. In the literature for direct human assistance, [6] proposed to set the velocity proportionally to the cable angle, [7] used an estimation of the operator force together with impedance control and [8] proposed a controller based on the cable angle and the cart velocity.

In contrast to the previous work, the controller proposed here automatically adapts the control gains to varying cable lengths. Additionally, these gains always lead to stable controllers for any given cable length. The control approach is based on backstepping, thus allowing simpler compensation scheme to varying parameters and nonlinear dynamics. Controllers for cooperation and autonomous modes are designed similarly to enable effective mode switch between control modes. Finally, the general behavior of the controller can be tuned by changing only two parameters (damping and natural frequency) which can be easily computed for any cable length.

B. CONTROL APPROACH

A controller based on a simplified cable dynamics with state space control is proposed here for interactive and autonomous motion. It is common in the literature to design a controller by considering both eqns. (7) and (8) at the same time [26]. However, the adaptive design is challenging and requires a precise estimation of the system parameters (such as the cart mass, the payload mass and the cable length). The proposed methodology is to use a backstepping approach to decouple the control problem into two controllers.

The first controller, referred to as the *main controller*, uses only eqn. (8) by considering the cart acceleration as the controlled variable. The second controller, referred to as the *cart controller*, uses only eqn. (7) to follow the required cart acceleration computed by the main controller. The controller design is then separated in two much simpler problems, which leads to several advantages. Indeed, the adaptation or compensation to varying parameters (cable length, cable extension velocity, damping, cart mass, and neglected terms from eqn. (2) such as $\dot{L}_p, \dot{\beta}_1, \dot{\theta}_1^2$ and viscous friction) is much simpler to perform with techniques such as feedforward, linearization or non-linear control when the systems equations are simpler. The estimation of the system parameters can be used to increase the controller performances but such estimates are not required and do not need to be as precise as with a classical state-space controller. The general control scheme is shown in Fig. 5 and the controllers are detailed in the next subsections. The robustness to errors in the measurement of the cable angle and angle velocities is important. The cable angle sensor design is thus significant. Additionally, remaining in a range of lower cable angles and cable angles velocities could also help to alleviate a potential robustness problem.

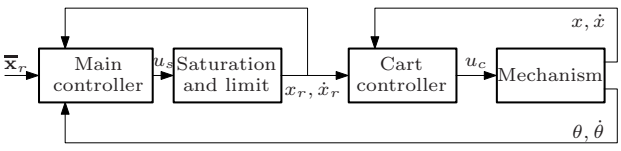

Fig. 5: Horizontal motions controller scheme.

C. MAIN CONTROLLER

The main controller uses eqn. (8) and the control objective is to compute the cart acceleration, $\ddot{x}$, that allows the system to reach the desired cart position, cart velocity, cable angle and cable angular velocity. Taking the Laplace transform of eqn. (8), one obtains

$$\ddot{X}(s) + g\theta_1(s) + s^2 L_p \theta_1(s) = 0 \tag{9}$$

where $\ddot{X}(s)$ and $\theta_1(s)$ are respectively the Laplace transform of $\ddot{x}(t)$ and $\theta_1(t)$

The state-space representation is therefore written as

$$\dot{\bar{\mathbf{x}}}_s = \mathbf{A}_s \bar{\mathbf{x}}_s + \mathbf{B}_s u_s \tag{10}$$

where $\bar{\mathbf{x}}_s$ is the state vector, u_s is the input scalar, $\mathbf{A}_s$ is a $n \times n$ state matrix, $\mathbf{B}_s$ is a $n \times m$ input matrix and where n is the number of states and m is the number of inputs.
In this case, one has $\bar{\mathbf{x}}_s = \begin{bmatrix} x & \dot{x} & \theta_1 & \dot{\theta}_1 \end{bmatrix}^T$, $u_s = \ddot{x}$, $m = 1$, $n = 4$ and

$$\mathbf{A}_s = \begin{bmatrix} 0 & 1 & 0 & 0 \\ 0 & 0 & 0 & 0 \\ 0 & 0 & 0 & 1 \\ 0 & 0 & \frac{-g}{L_p} & 0 \end{bmatrix} \quad \text{and} \quad \mathbf{B}_\mathrm{s} = \begin{bmatrix} 0 \\ 1 \\ 0 \\ \frac{-1}{L_p} \end{bmatrix}. \tag{11}$$

The control law is written as

$$u_s = \mathbf{K}_r \mathbf{e} \tag{12}$$

where

$$\boldsymbol{K}_r = \begin{bmatrix} K_x & K_v & -K_\theta & -K_{\theta p1} \end{bmatrix} \tag{13}$$

and

$$\boldsymbol{e} = \bar{\mathbf{x}}_r - \bar{\mathbf{x}}_s \tag{14}$$

where $\bar{\mathbf{x}}_r = \begin{bmatrix} x_r & \dot{x}_r & \theta_{1r} & \dot{\theta}_{1r} \end{bmatrix}^T$ are respectively the reference cart position and velocity and the reference cable angle position and velocity. In this problem, $\dot{x}_r$, θ_{1r} and $\dot{\theta}_{1r}$ are set to zero.

The cable length could be varied to stabilize cable oscillations but it is preferred to leave the cable length independent from the oscillations and it is thus not considered as a controlled variable for the mentioned control objectives. The cable length is considered constant over a time step in the model.

D. CART CONTROLLER

The cart controller uses eqn. (7) to follow the required cart acceleration obtained from the main controller. Since acceleration control is not practical, position or velocity control can be used. The discrete desired velocity to obtain the desired acceleration is obtained with a zero-order-hold integration, namely

$$\begin{aligned} \ddot{x}_d(k) &= u_s = \mathbf{K}_r \mathbf{e} \\ \dot{x}_d(k) &= \dot{x}_d(k-1) + \ddot{x}_d(k) T_s \end{aligned} \tag{15}$$

while the position is obtained by integrating once more:

$$x_d(k) = x_d(k-1) + \dot{x}_d(k-1) T_s + \frac{1}{2} \ddot{x}_d(k) T_s^2 \tag{16}$$

where T_s is the sampling period, k is the time step and x_d, $\dot{x}_d$ and $\ddot{x}_d$ are respectively the main controller required position, velocity and acceleration as shown in Fig. 5. This integration method, to achieve acceleration control, is used in other applications such as admittance control [11], [31].

The position or velocity can then be controlled with classical controllers such as a PID or computed-torque compensation (using for instance eqns. (2) and (3). Figure 5 presents the general control scheme where u_c is the command output from the cart controller. The limit and saturation block is used for safety such as virtual walls and for velocity and acceleration limitations.

E. COOPERATION MODE

In the cooperation mode, the operator is free to move the payload as desired and there is then no reference position, leading to $K_x = 0$. A state-space controller is proposed here. The characteristic polynomial of the system is obtained with:

$$\det\left[\mathrm{s}\boldsymbol{I} - \boldsymbol{A_s} + \boldsymbol{B_s K_r}\right] \tag{17}$$

where $\mathbf{I}$ is the $n \times n$ identity matrix, which leads to:

$$\Delta_c = \frac{s^3 L_p + s^2(K_{\theta p1} + K_v L_p) + s(g + K_{\theta 1}) + K_v g}{L_p}. \tag{18}$$

The transfer function of angle θ_1 to a cable angle initial condition $\theta_1(0)$ is then written as

$$\theta_1(s)/\theta_1(0) = (s + K_v)s/\Delta_c \tag{19}$$

The proposed methodology is to use adaptive pole placement by placing the poles to:

$$(s + p_1)(s^2 + 2\zeta_1 \omega_{n1} s + \omega_{n1}^2) \tag{20}$$

where p_1 is a real pole and where ω_{n1} and ζ_1 are the natural frequency and damping related to the complex poles. The proposed controller only uses the gains K_v and $K_{\theta 1}$ while K_x and $K_{\theta p1}$ (gain on the angular velocity signal) are set to zero.

Equating eqns. (18) and (20) and rearranging leads to:

$$\begin{aligned} p_1 &= \frac{2g\zeta_1\omega_{n1}}{-g + \omega_{n1}^2 L_p} \\ K_v &= \frac{p_1 \omega_{n1}^2 L_p}{g} \\ K_{\theta 1} &= (\omega_{n1}^2 - g/L_p + 2\zeta_1\omega_{n1} p_1) L_p \end{aligned} \tag{21}$$

where $\omega_{n1} > \sqrt{\frac{g}{L_p}}$ and ζ_1 are design parameters. The control gains are thus obtained and can be computed for any cable length.

As previously described and shown in Fig. 5, these gains help to compute the required cart acceleration to reach the control objectives. The cart controller is then used to follow the desired motion. From the characteristic polynomial of the system (eqn. 18), it can be observed that the poles depend on the control gains. Because the control gains are designed by placing the poles (eqn. (20)), the latter are necessarily negative for any cable lenght, given that $\omega_{n1} > \sqrt{\frac{g}{L_p}}$ and $\zeta_1 \geq 0$ and the controller is thus stable for any given cable length.

While the latter controller does not use the control gain $K_{\theta p1}$, it is easy to obtain similar equations while considering this gain. Using the gain $K_{\theta p1}$ may make the system more intuitive since it allows the cart to move not only in accordance to the cable angle but also to its angular velocity. This gain can be used or not, depending on the quality of the signal obtained for the time derivative of the cable angle and the designer choice.

F. AUTONOMOUS MODE

In the autonomous mode, K_x is used to prescribe the cart position. The control gain $K_{\theta p1}$ can also be used or not, depending on the designer's choice and the quality of the cable angle derivative signal. An adaptive controller based on pole placement and state space control using $K_{\theta p1}$ is proposed here.

Similarly to the cooperation mode, the system characteristic polynomial is written as:

$$\Delta_a = \frac{\begin{bmatrix} s^4 L + s^3(K_{\theta p1} + K_v L_p) \\ + s^2(g + K_{\theta 1} + K_x L_p) + s(K_v g) + K_x g \end{bmatrix}}{L_p}. \tag{22}$$

The transfer function from the angle θ_1 to a cable angle initial condition $\theta_1(0)$ is then written as

$$\frac{\theta_1(s)}{\theta_1(0)} = \frac{(s^3 L_p + s^2 K_v L_p + K_{\theta p1} + s L_p K_x)}{\Delta_a L_p} \tag{23}$$

and the transfer function of the position x of the cart in response to a reference position x_r is written as

$$X(s)/X_r(0) = K_x(s^2 L_p + g)/(\Delta_a L_p) \tag{24}$$

There is a compromise between the cart position trajectory and the cable oscillation cancellation. The proposed methodology is to use adaptive pole placement by placing the poles to:

$$(s + p_1)^2(s^2 + 2\zeta_1\omega_{n1} + \omega_{n1}^2). \tag{25}$$

Equating the poles from equations eqns.(22) and (25) and rearranging, one obtains

$$\begin{aligned} K_x &= \omega_{n1}^2 p_1^2 L_p/g \\ K_v &= 2\omega_{n1} p_1 L_p(\omega_{n1} + \zeta_1 p_1)/g \\ K_{\theta 1} &= (\omega_{n1}^2 + 4\zeta_1\omega_{n1} p_1 + p1^2 - K_x - g/L_p)L_p \\ K_{\theta p1} &= (2\zeta_1\omega_{n1} + 2p1 - K_v)L_p \end{aligned} \tag{26}$$

where $\omega_{n1} \geq \sqrt{\frac{g}{L_p}}$ and ζ_1 are design parameters and p_1 is heuristically chosen to be equal to ω_{n1} in order to lie on the same complex circle as the other poles. Using a pair of complex poles and two equal real poles is a design choice but other options are possible. The state space controller gains that adapt to any cable length are thus obtained. As previously described and shown in Fig. 5, these gains help to compute the required cart acceleration to reach the control objectives. The cart controller is then used to follow the desired motion. The operator can still push the payload in autonomous mode: the cart position moves in the direction desired by the operator while being attracted to its reference position and controlling cable oscillations.

Finally, when switching from a given mode (cooperation or autonomous) to another, large accelerations and jerks may be obtained and bumpless control transfer must then be considered. Because both cooperation and autonomous modes shares the same controller design methodology, mode transfer is easier to implement.

V. VERTICAL MOTION CONTROL

This section describes the vertical assistance mode. In the litterature, a force sensor is normally placed in line with the cable in order to measure the force applied by the operator and to allow him/her to place his hands anywhere on the payload [9], [3], [8]. However, the force signal is affected by the dynamical effects of the payload [32], [8] which must then be compensated for in order to obtain a good estimation of the force applied by the operator [9], [10]. The resulting signal is then used as an input to a force control scheme such as admittance control [11] to assist the operator in moving the payload [8], [12].

In contrast to the previous work, the contribution of this section is the proposition of novel methods to estimate more precisely the dynamical effects affecting the force signal. The objective is to obtain better estimation of the payload mass and of the force applied by the operator in order to reduce the force required by the operator to move the payload.

A. ACCELERATION ESTIMATION

From eqn. (4), the force measured at the load cell can be written as

$$\begin{aligned} f_L &= f_H + m(\ddot{X}_c \cos\beta_1 \sin\theta_1 + \ddot{L}_p - L_p\dot{\beta}_1^2 \\ &\quad -L_p\dot{\theta}_1^2 \cos^2\beta_1 + \ddot{Y}_c \sin\beta_1 - g\cos\beta_1\cos\theta_1) \\ &= f_H + m a_p \end{aligned} \tag{27}$$

where f_H is the operator force and a_p is the payload acceleration. Three possible methods to estimate the payload acceleration are now described. The accelerometer method was proposed in [10], [33] while the individual compensation method and the fusion method are proposed in this paper.

1) ACCELEROMETER METHOD: Different variants of the accelerometer method are proposed in the literature [10], [33]. A first solution consists in placing a rotational accelerometer on the winch shaft to measure the motor angular acceleration. The cable length acceleration can then easily be determined. However, this solution only provides an estimation of the cable length acceleration and thus several terms appearing in eqn.(27) are not accounted for. A second solution consists in placing a linear accelerometer in line with the cable as shown in Fig. 6. However, the acceleration estimation is obtained at the accelerometer position, L_a, while the acceleration at the payload position, L_p, is required. In practice, the accelerometer is often relatively far from the payload's centre of mass and the compensation of the dynamical effects is thus not very accurate. The payload estimation at the payload position cannot be simply obtained by multiplying the accelerometer signal by a given factor since the signal only outputs the overall results of all the dynamical effects. Additionally, the accelerometer signal is often noisy, can drift with time or temperature and it is not necessarily reliable if impacts occur.

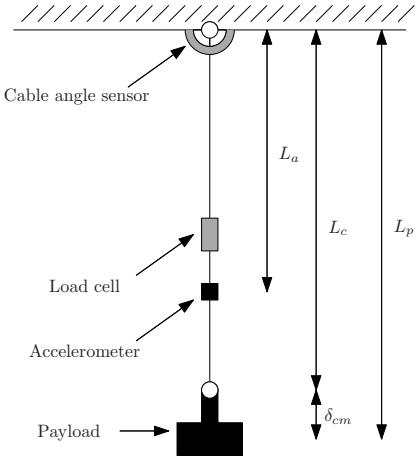

Fig. 6: Description of the cable length parameters.

2) INDIVIDUAL METHOD: The individual method proposed here consists in computing each term of eqn. (27) individually, thereby allowing to estimate the acceleration at the payload position. The estimation is not subject to drift as with the accelerometer method but it is more subject to noise, especially because of acceleration estimations.

From eqn. (27), several measurements are needed, namely:

- **Cable angles θ_1 and θ_2 (from which β_1 is inferred)**: These angles are obtained from the cable angle sensor, as presented in section II-A.
- **Cable angular velocities $\dot{\theta}_1$ and $\dot{\theta}_2$ (from which $\dot{\beta}_1$ is inferred)**: These angular velocities are obtained from the cable angle derivatives. An angular velocity sensor (such as a gyroscope) could also be placed on the cable angle sensor shafts.
- **Cable length L**: Obtained with a position sensor on the winch motor shaft (in this work a Hall-effect sensor and an incremental encoder signal are fused). The payload position, L_p, is obtained with:

$$L_p = L_c + \delta_{cm} \tag{28}$$

  where L_c is the cable length and δ_{cm} is an estimation of the distance between the payload centre of mass and the payload attachment point, as shown in Fig. 6.
- **Cable vertical acceleration $\ddot{L}_p$**: Obtained from the second derivative of the cable length measurement or from the trajectory's desired acceleration. In our implementation, a fusion of these signals is used. Alternatively, a rotational accelerometer or a gyroscope could also be placed on the winch motor shaft.
- **Cart acceleration $\ddot{X}_C$ and $\ddot{Y}_C$**: Obtained from the second derivative of the position or from the trajectory's desired acceleration. In our implementation, a fusion of these signals is used. Alternatively a rotational accelerometer or a gyroscope mounted on the motor shafts or linear accelerometers placed on the cart could also be used.

The acceleration estimation obtained with the individual method, $\hat{a}_I$, is then computed by substituting all the above measurements and estimations in eqn. (27).

3) FUSION METHOD: The fusion method consists in fusing the accelerometer and the individual method to capture the advantages of both methods while minimizing their drawbacks. The acceleration estimation at the accelerometer position, L_a, is first obtained independently from the accelerometer and by the individual method. Both estimations are then fused at this position using linear data reconciliation [34] with:

$$E_1 + E_2 + E_3 + E_4 = E_5 \tag{29}$$

where

$$\begin{aligned} E_1 &= \ddot{L}_a \\ E_2 &= -L_a\dot{\beta}_1^2 - L_a\dot{\theta}_1^2\cos^2\beta_1 \\ E_3 &= -g\cos\beta_1\cos\theta_1 \\ E_4 &= \ddot{X}_c\cos\beta_1\sin\theta_1 + \ddot{Y}_c\sin\beta_1 \\ E_5 &= a_{acc} \end{aligned} \tag{30}$$

and where $E_5 = a_{acc}$ is the accelerometer signal and E_1 to E_4 are obtained with the individual method. The linear data reconciliation method from [34] allows to define different confidence factors for each parameter E_i. The outputs are reconciled values of each parameter E_i and are referred to as $\hat{E}_i$. The estimation of the acceleration at the payload position is then obtained with:

$$\hat{a}_F = \hat{E}_1 + \hat{E}_2\frac{L_p}{L_a} + \hat{E}_3 + \hat{E}_4 \tag{31}$$

where $\hat{a}_F$ is the payload acceleration estimation provided by the fusion method. It would also be possible to use other set of sensors (for example an assembly of accelerometers) and fuse them together.

B. FLOAT MODE

The vertical assistance mode proposed here (also called float mode) uses the estimation of the force applied by the operator together with admittance control. The force applied by the operator must first be obtained from the load cell signal and from eqn. (27) with:

$$\hat{f}_H = f_L - \hat{m}_0\hat{a}_F \tag{32}$$

where $\hat{a}_F$ is the payload acceleration estimation obtained from the fusion method, f_L is the load cell signal and $\hat{m}_0$ is the payload mass estimation prior to entering the float mode. This estimation of the payload mass is thus very important. The estimation is based on an online identification technique [35] using the following equation (the human force is considered to be zero during the calibration):

$$f_L = \hat{m}_0\hat{a}_F. \tag{33}$$

The payload mass estimation can also be used to determine if the device is loaded or if the payload maximum limit is reached. The payload acceleration estimation used for the compensation of the dynamical effects is thus not only important for the operator force estimation but also for the payload mass estimation.

Once the force applied by the operator is obtained, a classic admittance control scheme is used to assist the operator in

moving the payload. The admittance force control scheme accepts a force as input, which is measured, and reacts with a displacement [36], [12]. More information about the design of admittance controllers and stability issues can be found in [11], [37]. The float mode controle scheme is shown in Fig. 7 while the general vertical control scheme is shown in Fig. 8.

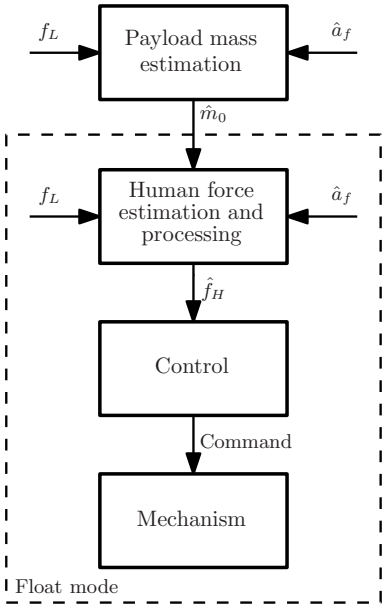

Fig. 7: General float mode control scheme.

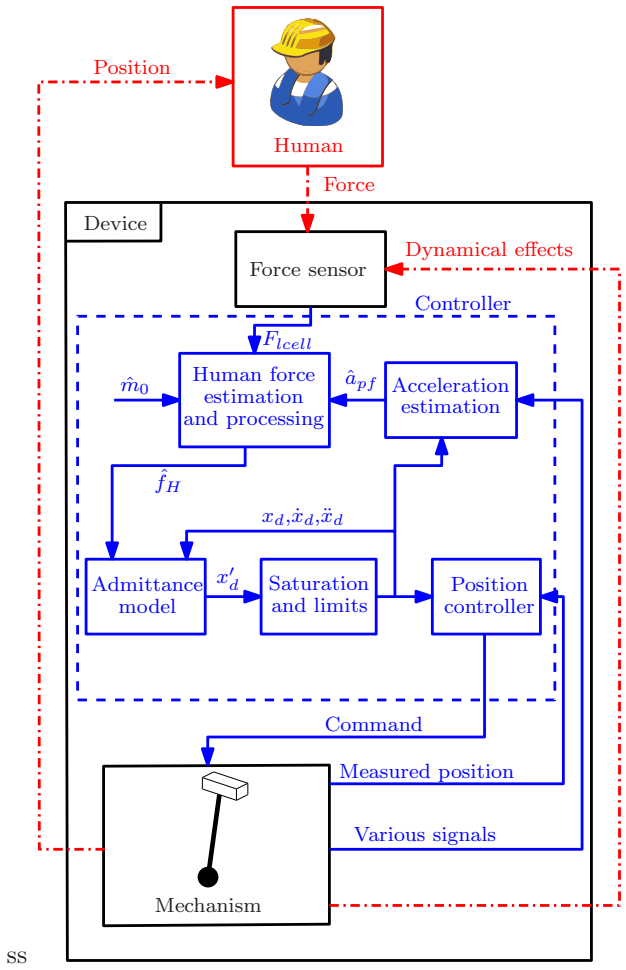

Fig. 8: Detailed vertical control scheme.

VI. EXPERIMENTATION

Experiments were performed using the industrial-scale gantry system shown in Fig. 1 [38]. The total moving mass is approximately $350kg$ in the direction of the X axis and $170kg$ along the Y axis. A winch using a DC motor and a pulley was used to produce the vertical motion. Additionally, a commercial Omega load cell (LC-111-200) and an accelerometer (ADXL-330) were mounted in line with the cable. The payload may vary between 0 and $45kg$ (a $45kg$ payload is used in the experiments). The horizontal workspace is $3.3m \times 2.15m$ while the vertical range of motion is $1m$. The controller is implemented on a real-time QNX computer with a sampling period of 2ms. The algorithms are programmed using Simulink/RT-LAB software. A video shows excerpts from the experiments.

A. HORIZONTAL MODE

1) COOPERATION MODE: The first experiment consisted in giving an impulse to the payload and to compare the response between the proposed controller and the method described in [6]. In order for the system to be intuitive to the human operator, the first objective is to limit the cable oscillations. Ideally, in response to an impulse, the cable should smoothly return to the vertical position in the least amount of time as possible. Figure 9 presents the comparison where L_p is the cable length and L_c is the cable length used by the controller. The solid blue line and the red dashed line are with the fixed parameters method proposed in [6]. The controller was designed for a cable length L_p of $2.5m$ (solid blue line). However, using the same control parameter with a cable length L_p of $1.2m$ result in an oscillatory response and can even lead to instability depending on the control gain and the actual cable length. The green dot-dashed line and the black dotted line are with the proposed controller with $\zeta_1 = 0.9$. Because the controller automatically computes stable control gains for varying cable lengths, the response is satisfactory for any cable length. The response time to stabilize below an angle of 0.25° are 2.35s (blue line) and 3.45s (red line) for the fixed case and are 2.12s (green) and 1.59s (black) for the adaptive case.

Two other experiments were conducted using the cooperation mode: a recovery from an impulse and motion assistance. The recovery from an impulse experiment consisted in giving a large impulse to the payload in order to test the controller's ability to bring the cable back to the vertical position. The results are shown in Fig. 10 where L_p is the cable length and L_c is the cable length used by the controller. Subfigures 10(a) to 10(c) show results from experiments with different cable lengths and damping ratios. Subfigure 10(d) shows results from an experiment in which L_c is different from L_p in order to test the controller's robustness to modelling and measurement errors. In all cases, the cable returns to the

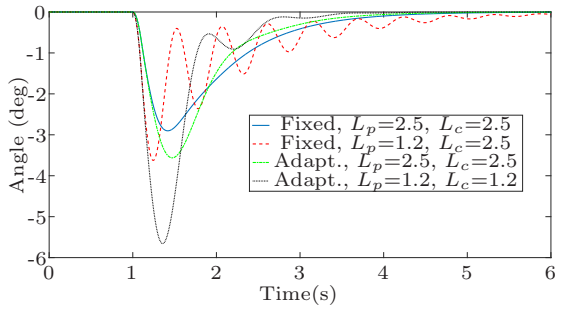

Fig. 9: Comparison between the proposed controller and a method described in the litterature for different cable lengths.

TABLE I: Required force for horizontal motion

Parameter	Unit	Value
Payload	kg	45
Force required for precise motion (0.2 m/s)	N	11
Force required for fast motion (0.6 m/s)	N	35

vertical position rapidly and smoothly. The second experiment, shown in Fig. 11, consisted in performing usual motions in order to assess the assistance to the operator. This figure gives information on the interaction with the assistive device by allowing to see the relation between the force applied by the human and the resulting system velocity and cable angle. The force applied by the operator was measured with an ATI force sensor (used only for the measurements and is not used by the controller). The required force with a $45kg$ payload (shown in Tab. I) for precise motions ($0.2m/s$) is $11N$ while the required force for fast motions ($0.6m/s$) is $35N$. Additionally, the system automatically brings the cable to the vertical position and thus the operator does not have to stop the payload.

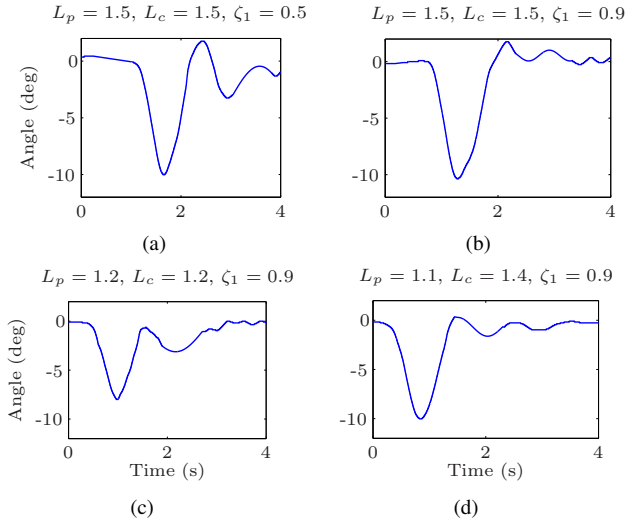

Fig. 10: Horizontal impulse experiment.

2) AUTONOMOUS MODE: The autonomous mode experiment consisted in prescribing a position while damping cable oscillations. The trajectory consisted in starting from $x = -0.3m$ to $x = 0.3m$. A first-order low pass filter

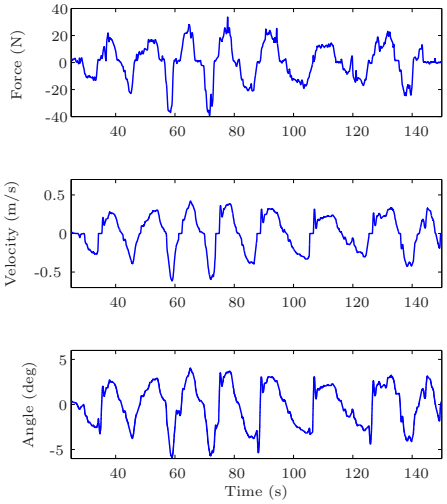

Fig. 11: Horizontal mode interaction experiment.

with a time constant of 0.8 was applied to prevent abrupt motions. Fig. 12 shows the experimental results. The first experiment was conducted using a control parameter ζ_1 of 0.9. The cable oscillations were kept to minimal values while the cart position motion was more jerky. The position response time (95%) was $3.74s$, the position overshoot was 0.8%, the angle response time (below 2°) was $1.49s$ and the angle RMS value was 1.72. The second experiment was conducted using a control parameter ζ_1 of 0.4. The cable oscillations were kept to medium values while the cart position motion was more or less jerky. The position response time (95%) was $3.79s$, the position overshoot was 8.6%, the angle response time (below 2°) was $2.83s$ and the angle RMS value was 2.73. The third experiment only considered the prescribed position without considering the cable angle. The cable oscillations were then really large while the cart position motion was very smooth. The position response time (95%) was $2.71s$, the position overshoot was 0.6%, the angle response time (below 2°) was not achieved in a decent time and the angle RMS value was 13.28. In summary, increasing ζ_1 allows to reduce the cable angle oscillations amplitude but, as a compromise, the cart position profile may be more jerky. In typical applications, it is desired to minimize the cable sway as much as possible and a higher value of ζ_1 is then preferred. In practice however, a high value of ζ_1 may require high cart accelerations, which can be too difficult for the controller or the mechanics to cope with. From our experiments, a ζ_1 value of 0.9 is recommended.

B. VERTICAL MODE

Two experiments were performed in order to test the vertical control mode: a motion assistance using the float mode and a payload mass estimation comparing the different acceleration estimation methods.

The results of the motion assistance are presented in Fig. 13 where the first subfigure shows the force applied by the operator. The force estimated from the load cell data is compared to the signal of an ATI 6-axis force/torque sensor placed on the payload. The second subfigure shows the resulting velocity. Table II shows the required forces for different motions.

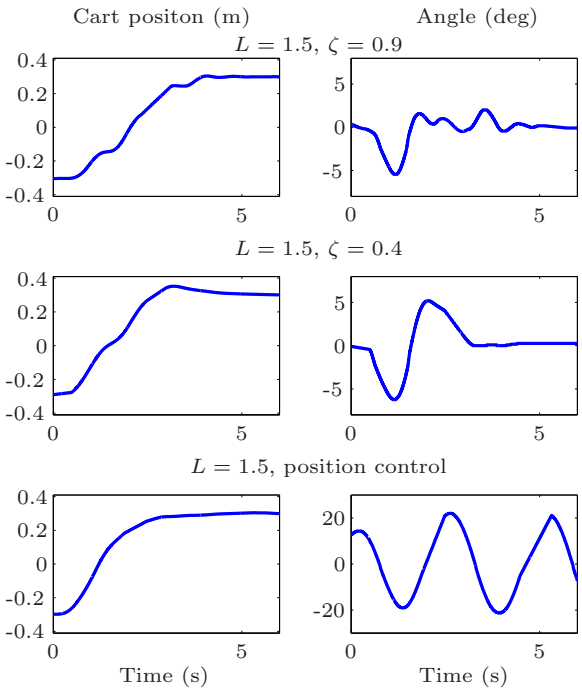

Fig. 12: Autonomous mode experiment.

TABLE II: Required force for vertical motion

Parameter	Unit	Value
Payload	kg	45
Force required for precise motion (0.2 m/s)	N	15
Force required for fast motion (0.6 m/s)	N	50

The second experiment consisted in estimating the payload mass in different situations. Figure 14 shows the load cell signal, f_L, and the payload mass estimated with the accelerometer, the individual and the fusion methods. The experiment is divided in three zones: in zone I slow autonomous vertical motions were performed; in zone II horizontal motions were performed to excite the dynamic terms; in zone III fast vertical autonomous motions were performed.

The performance of the individual method is better than that of the accelerometer method when the payload sways (zone II). However, the performance of the accelerometer method is better than that of the proposed individual method in the presence of vertical motions (zone I and III). The proposed fusion method, taking advantage of the above two methods, leads to better overall results and to reduced maximal deviation from the expected mass. For this experimentation, the root mean square (RMS) value of the error was 0.0556 for the fusion method, 0.0585 for the individual method and 0.1116 for the accelerometer method. In our experiment, L_a was $0.9m$ and L_p was $1.25m$. In an industrial application, the payload's centre of mass is typically farther from the accelerometer and the improvement should then be even greater. Similar experiments have shown that the error in the estimation of the operator force was reduced by 40% when using the fusion method.

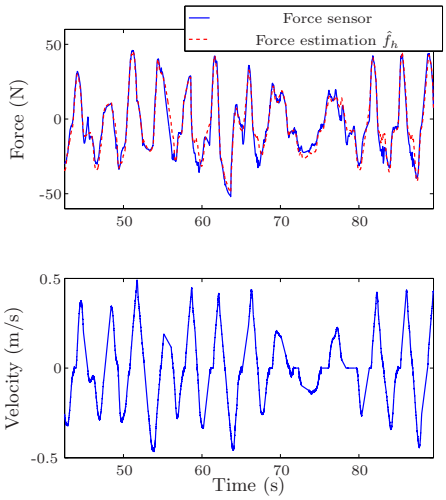

Fig. 13: Force and velocity with float mode cooperation.

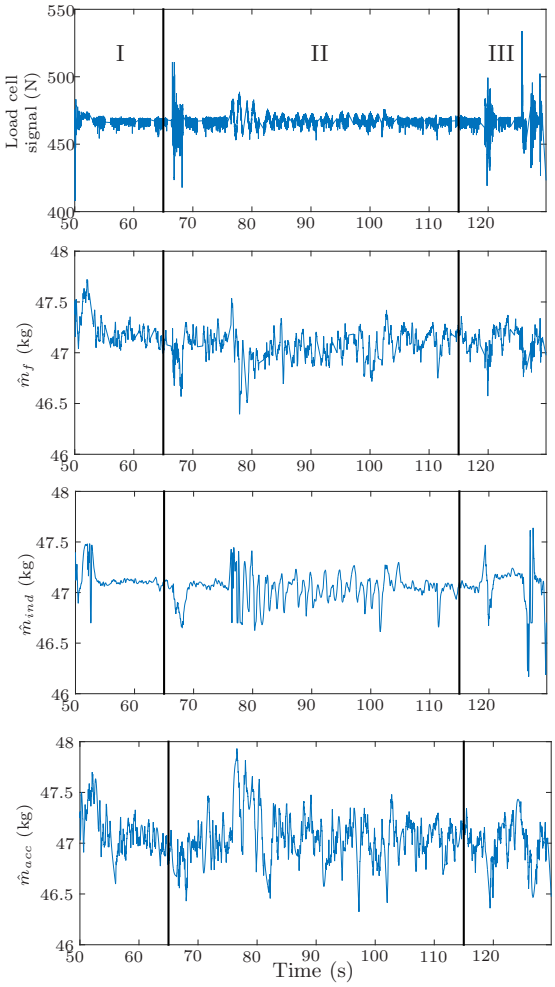

Fig. 14: Load cell signal and mass estimation with the fusion method, the individual method and the accelerometer method.

CONCLUSION

This paper proposed a cable-suspended human augmentation system. A cable angle sensor designed to be precise, robust and low-cost was first proposed. The reliability and precision of this sensor was found to be of the utmost importance for the controller performance, both for horizontal and vertical motions. While a simple dynamic model was sufficient for the horizontal controller, the complete model proved to be very important for the performance of the vertical controller. Horizontal and vertical controllers adapting automatically to any cable lengths were designed for direct human assistance. Dynamical effects affecting the force sensor signal were then presented. A fusion between the state-of-the-art accelerometer method and a new proposed individual method led to better performances. Finally, experiments were performed on an industrial-scale industrial system.

While a cable-suspended system can be used in many applications, some tasks are not possible since the payload's centre of mass must necessarily be aligned with the cable. Future work will focus on the development of hands-on-payload solutions that do not suffer from this drawback.

ACKNOWLEDGMENT

This work was supported by The Natural Sciences and Engineering Research Council of Canada (NSERC) as well as by the Canada Research Chair Program and General Motors (GM) of Canada.

REFERENCES

[1] A. Bicchi, M. A. Peshkin, and J. E. Colgate, "Safety for physical human-robot interaction," in *Springer Handbook of Robotics*, 2008.

[2] J. E. Colgate, M. Peshkin, and S. H. Klostermeyer, "Intelligent assist devices in industrial applications: a review," in *Proceedings of the International Conference on Intelligent Robots and Systems*, Las Vegas, October 2003, pp. 2516–2521.

[3] H. Kazerooni, "Exoskeletons for human performance augmentation," in *Springer Handbook of Robotics*, 2008, pp. 773–793.

[4] M. Peshkin, "Non-contacting sensors ," 1999, US patent 6,668,668.

[5] S. Kahlman, "Arrangement for controlling the direction of movement of a load hoist trolley ," 1991, US patent 5,350,075.

[6] E. Colgate, P. Decker, S. Klostermeyer, A. Makhlin, D. Meer, J. Santos-munne, M. Peshkin, and M. Robie, "Methods and apparatus for manipulation of heavy payloads with intelligent assist devices," 2008, US Patent 7,185,774.

[7] J. Wen, D. Popa, G. Montemayor, and P. Liu, "Human assisted impedance control of overhead cranes," in *Proceedings of the IEEE International Conference on Control Applications*, 2001, pp. 383 –387.

[8] A. Niinuma, T. Miyoshi, K. Terashima, and Y. Miyashita, "Evaluation of effectiveness of a power-assisted wire suspension system compared to conventional machine," in *International Conference on Mechatronics and Automation*, Aug 2009, pp. 369–374.

[9] T. Miyoshi and K. Terashima, "Control of power-assisted crane system using direct manual manipulation," in *Proceedings of the IEEE International Conference on Control Applications*, vol. 1, 2004, pp. 38–44.

[10] W. Wannasuphoprasit, J. Colgate, D. Meer, and M. Peshkin, "Method and apparatus for a high-performance hoist," 2001, US Patent 6,241,462.

[11] A. Lecours, B. Mayer-St-Onge, and C. Gosselin, "Variable admittance control of a four-degree-of-freedom intelligent assist device," in *Proceedings of the 2012 IEEE International Conference on Robotics and Automation (ICRA)*, May 2012, pp. 3903–3908.

[12] F. Dimeas, P. Koustoumpardis, and N. Aspragathos, "Admittance neuro-control of a lifting device to reduce human effort," *Advanced Robotics*, vol. 27, no. 13, pp. 1013–1022, 2013.

[13] T. Noro, Y. Katsuda, T. Miyoshi, and K. Terashima, "Estimation method of operating force using an extended Kalman filter based on ground reaction force and human behavior," in *International Symposium on Micro-NanoMechatronics and Human Science (MHS)*, 2014, pp. 1–4.

[14] M. K. Taylor, "Pendant-responsive crane control ," 2001, US patent 6,575,317.

[15] B. B. Laundry, L.-t. Liu, G. Montemayor, D. O. Popa, M. K. Taylor, and J. T. Wen, "Crane control system ," 2002, US patent 6,796,447.

[16] Y. Kim, K. Hong, and S. Sul, "Anti-sway control of container cranes: Inclinometer, observer, and state feedback," *International Journal of Control, Automation, and Systems*, vol. 2, no. 4, pp. 435–449, 2004.

[17] K. L. Sorensen, W. Singhose, and S. Dickerson, "A controller enabling precise positioning and sway reduction in bridge and gantry cranes," *Control Engineering Practice*, vol. 15, no. 7, pp. 825 – 837, 2007.

[18] J. Huang, X. Xie, and Z. Liang, "Control of bridge cranes with distributed-mass payload dynamics," *Mechatronics, IEEE/ASME Transactions on*, vol. 20, no. 1, pp. 481–486, Feb 2015.

[19] G. Stepan, A. Toth, L. Kovacs, G. Bolmsjo, G. Nikoleris, D. Surdilovic, A. Conrad, A. Gasteratos, N. Kyriakoulis, D. Chrysostomou *et al.*, "Acroboter: a ceiling based crawling, hoisting and swinging service robot platform," in *Beyond gray droids: domestic robot design for the 21st century workshop at HCI*, vol. 2009, no. 3, 2009, pp. 2–5.

[20] S. Ohtomo and T. Murakami, "Estimation method for sway angle of payload with reaction force observer," in *IEEE International Workshop on Advanced Motion Control (AMC)*, March 2014, pp. 581–585.

[21] A. Lecours, S. Foucault, T. Laliberte, C. Gosselin, B. Mayer-St-Onge, D. Gao, and R. Menassa, "Movement system configured for moving a payload in a plurality of directions," 2015, US Patent 8,985,354.

[22] J. M. Wiitala and M. M. Stanišić, "Design of an overconstrained and dextrous spherical wrist," *Journal of Mechanical Design*, vol. 122, no. 3, pp. 347–353, 2000.

[23] B. Adelstein and M. Rosen, "Design and implementation of a force reflecting manipulandum for manual control research," in *ASME Winter Annual Meeting*, Anaheim, California, 1992.

[24] P. Belanger, P. Dobrovolny, A. Helmy, and X. Zhang, "Estimation of angular velocity and acceleration from shaft-encoder measurements," *The International Journal of Robotics Research*, vol. 17, no. 11, pp. 1225–1233, 1998.

[25] H.-H. Lee, "Modeling and control of a three-dimensional overhead crane," *Journal of Dynamic Systems, Measurement, and Control*, vol. 120, no. 4, pp. 471–476, 1998.

[26] A. Piazzi and A. Visioli, "Optimal dynamic-inversion-based control of an overhead crane," *IEEE Proceedings-Control Theory and Applications*, vol. 149, no. 5, pp. 405–411, 2002.

[27] M. Mokhtari, N. Golea, and S. Berrahal, "The observer adaptive back-stepping control for a simple pendulum," *AIP Conference Proceedings*, vol. 1019, no. 1, pp. 85–90, 2008.

[28] K. A. F. Moustafa, "Reference trajectory tracking of overhead cranes," *Journal of Dynamic Systems, Measurement, and Control*, vol. 123, no. 1, pp. 139–141, 2001.

[29] J. Collado, R. Lozano, and I. Fantoni, "Control of convey-crane based on passivity," in *Proceedings of the American Control Conference*, vol. 2, 2000, pp. 1260–1264.

[30] H. Lee and S. Jung, "Balancing and navigation control of a mobile inverted pendulum robot using sensor fusion of low cost sensors," *Mechatronics*, vol. 22, no. 1, pp. 95 – 105, 2012.

[31] C. Gosselin, A. Lecours, T. Laliberte, and M. Fortin, "Design and experimental validation of planar programmable inertia generators," *The Intern. Journal of Robotics Research*, vol. 33, no. 4, pp. 489–506, 2013.

[32] E. Sariyildiz and K. Ohnishi, "An adaptive reaction force observer design," *Mechatronics, IEEE/ASME Transactions on*, vol. 20, no. 2, pp. 750–760, April 2015.

[33] R. Devos, "Hoist controls with compensation for dynamic effects ," 2008, US patent 7,810,791.

[34] S. Narasimhan and C. Jordache, *Data Reconciliation & Gross Error Detection-An Intelligent Use of Process Data*. Elsevier, 2000.

[35] L. Ljung and T. Soderstrom, *Theory and Practice of Recursive Identification*. MIT Press, 1983.

[36] H. Woo and K. Kong, "Controller design for mechanical impedance reduction," *Mechatronics, IEEE/ASME Transactions on*, vol. 20, no. 2, pp. 845–854, April 2015.

[37] A. Lecours and C. Gosselin, "Computed-torque control of a four-degree-of-freedom admittance controlled intelligent assist device," in *Experimental Robotics*, ser. Springer Tracts in Advanced Robotics. Springer International Publishing, 2013, vol. 88, pp. 635–649.

[38] C. Gosselin, T. Laliberte, B. Mayer-St-Onge, S. Foucault, A. Lecours, V. Duchaine, N. Paradis, D. Gao, and R. Menassa, "A friendly beast of burden: A human-assistive robot for handling large payloads," *IEEE Robotics Automation Magazine*, vol. 20, no. 4, pp. 139–147, Dec 2013.